Supporting Information
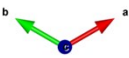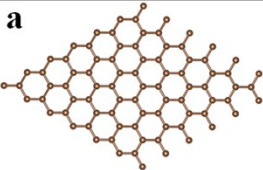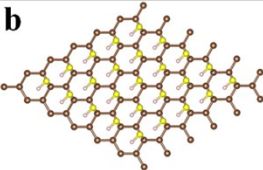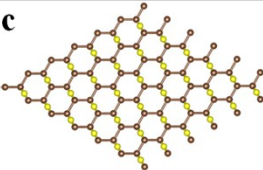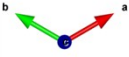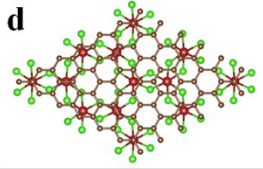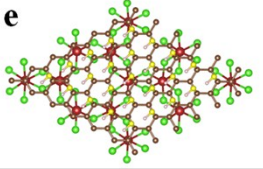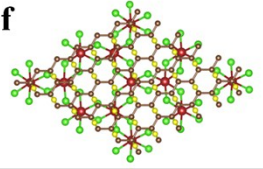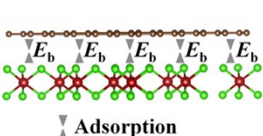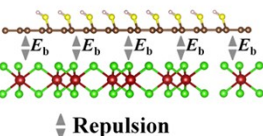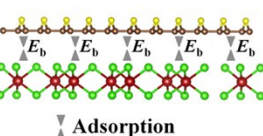
Strong Anchoring Effect of Ferric Chloride-Graphite Intercalation Compounds (FeCl₃-GICs) with Tailored Epoxy Groups for High-Capacity and Stable Lithium Storage

Chengzhi Zhang,[a,b] Jianmin Ma,[c] Fei Han,*[a,b] Hongbo Liu,[a,b] Fuquan Zhang,[a,b] Changling Fan,[a,b] Jinshui Liu,*[a,b] and Xuanke Li*[a,b,c]
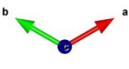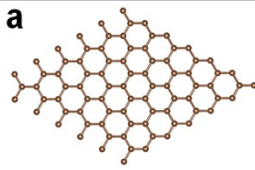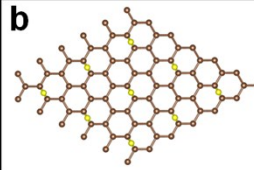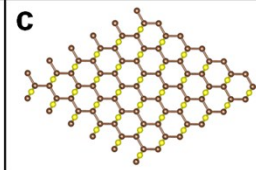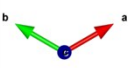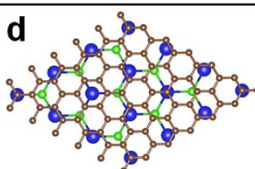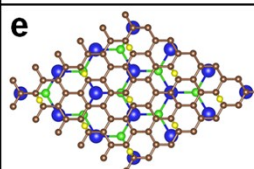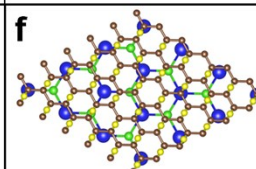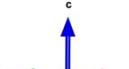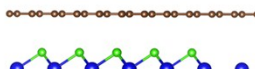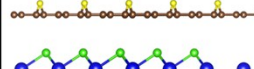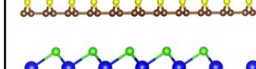
[a] *College of Materials Science and Engineering, Hunan University, Changsha 410082, China*

[b] *Hunan Province Key Laboratory for Advanced Carbon Materials and Applied Technology, Hunan University, Changsha, Hunan, 410082, China*

[c] *School of Physics and Electronics, Hunan University, Changsha 410082, China*

	G	OG (hydroxyl)	OG2	
	a	**b**	**c**	Top view
	FeCl$_3$/G	FeCl$_3$/OG (hydroxyl)	FeCl$_3$/OG2	○ O atom
	d	**e**	**f**	Top view
	Adsorption	Repulsion	Adsorption	Side view
Binding energy	E_b=0.05875eV	E_b=-0.88125eV	E_b=0.21625eV ✓	○ H atom

Figure S1. The building blocks of (a) pristine graphite (G), and oxidized graphite (OG) with (b) fully oxidized by hydroxyl groups, and (c) fully oxidized by epoxy groups (OG2). (d–f) Top view and side view of the FeCl$_3$/G, FeCl$_3$/OG (hydroxyl) and FeCl$_3$/OG2 structures.

	G	OG1	OG2	
	a	**b**	**c**	Top view
	LiCl/G	LiCl/OG1	LiCl/OG2	○ O atom
	d	**e**	**f**	Top view
				Side view
Binding energy	$E_b = -0.18443$ eV	$E_b = 0.11248$ eV	$E_b = 0.30667$ eV	● Li atom

Figure S2. The building blocks of (a) Graphite layer (G), and OG with (b) low content of epoxy functional groups (OG1), and (c) fully oxidized by epoxy groups (OG2). (d–f) top view and side view of the LiCl/G, LiCl/OG1 and LiCl/OG2 structures.

The adsorption energy per LiCl unit (E_b) for the thermodynamic stability of a graphite monolayer with the monolayer LiCl to make LiCl/(O)G composite, is defined as:

$$E_b = (E_{LiCl} + E_{(O)G} - E_{LiCl/(O)G})/n$$

where E_{LiCl}, $E_{(O)G}$ and $E_{LiCl/(O)G}$ represent the total relaxation energies of monolayer LiCl, (O)G and LiCl/(O)G composite, respectively. n is the total number of LiCl unit in the supercell. The result shows that the interaction binding energies between LiCl and graphite monolayer increase with the increase of the content of the epoxy groups.

Therefore, the epoxy groups on the graphite layer are in favor of chemically anchoring LiCl, further preventing the dissolution of chlorides in electrolytes during electrochemical cycling.
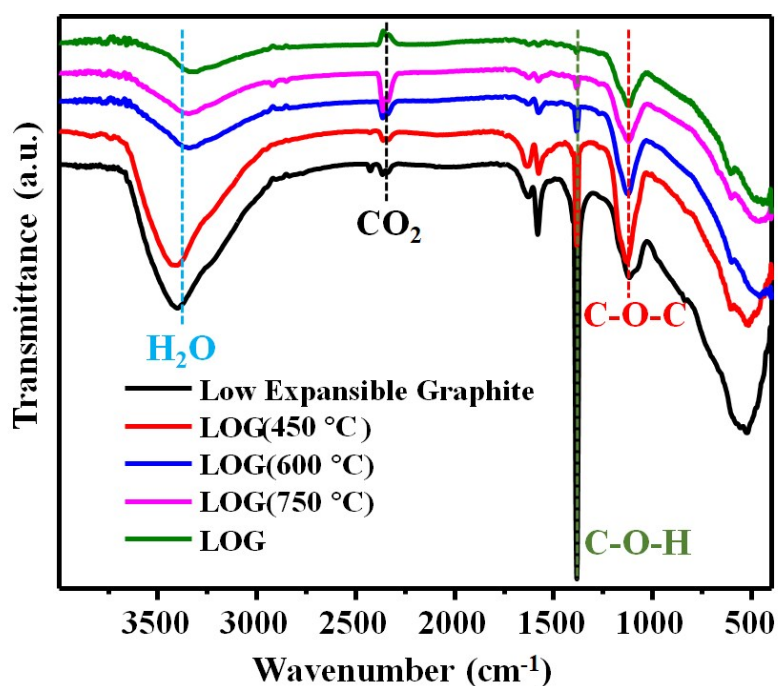
Figure S3. FT-IR spectra of low oxidized graphite and LOGs with different heat-treated temperatures of 450 °C, 600 °C, 750 °C and 900 °C at air for 12 sec, respectively.
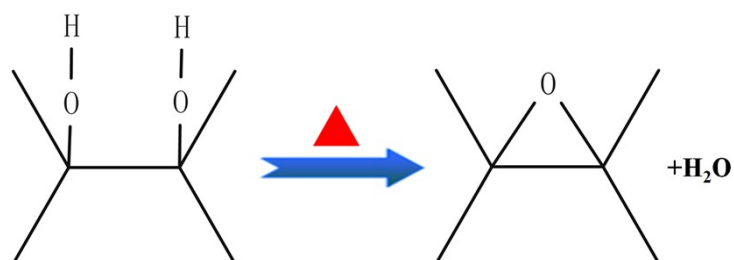
Figure S4. The conversion reaction between epoxy and hydroxyl on a graphite monolayer.[1]

To controllably produce epoxy groups on the graphite layers, previous works discovered that the hydroxyl groups formed during an oxidization process can be gradually transformed into the epoxy groups at a high temperature owing to the higher thermostability of the epoxy groups. A similar result in this work also prove the above viewpoint on the basis of the FT-IR spectra of low oxidized graphite and its derivatives (LOGs) heated at different temperatures from 450 to 900 °C (Figure S3 and S4). The result shows that the epoxy group is the main component of oxygen groups after a heating treatment at 900 °C.
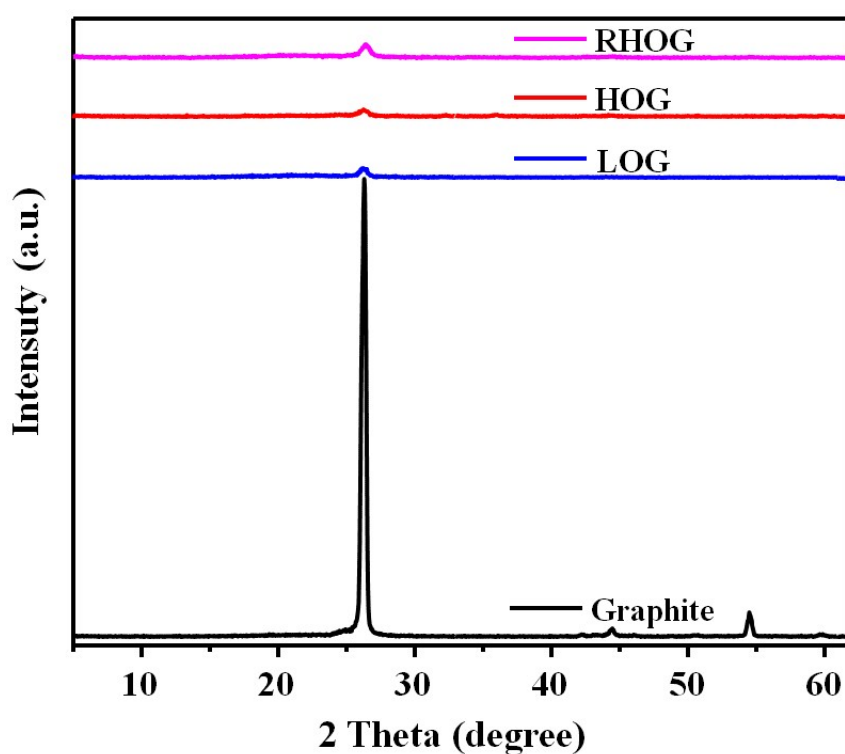
Figure S5. Wide-angle XRD patterns of pristine graphite, LOG, HOG and RHOG hosts.
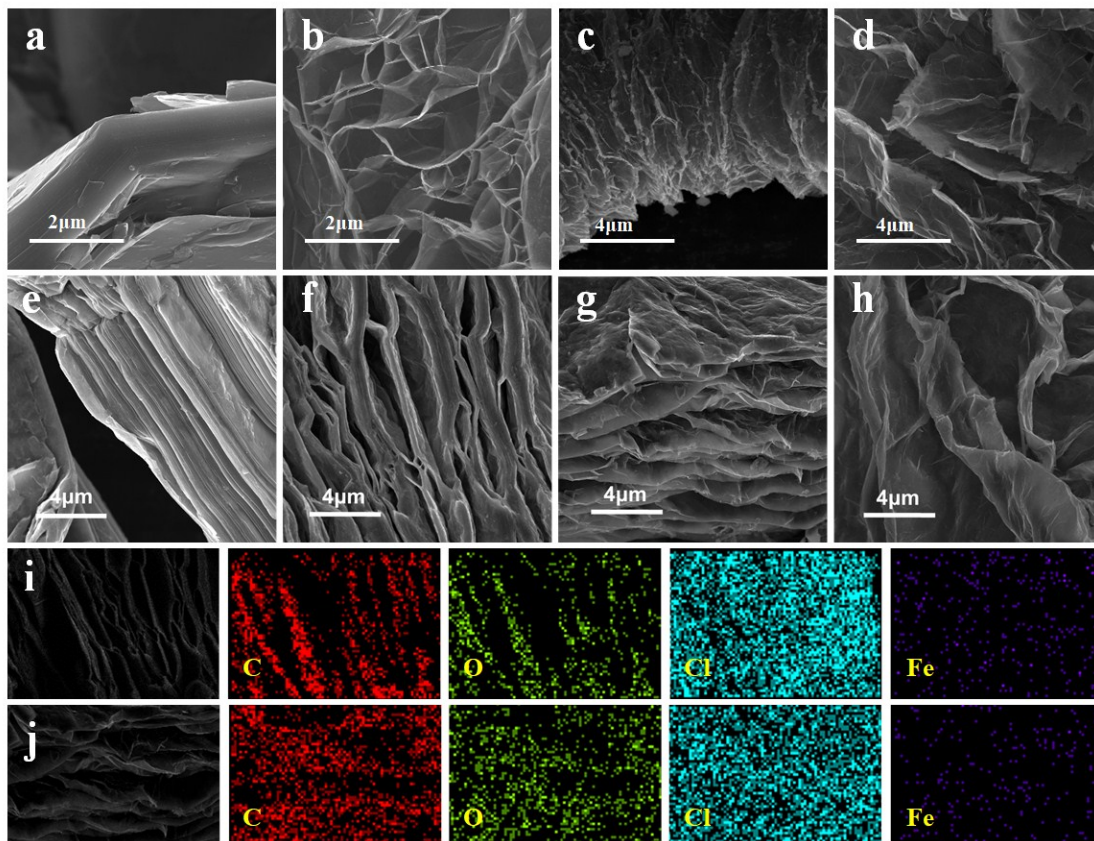
Figure S6. SEM images of (a,e) pristine graphite and its $FeCl_3$-GIC, (b,f) LOG and its $FeCl_3$-LOGIC, (c,g) HOG and its $FeCl_3$-HOGIC, (d,h) RHOG and its $FeCl_3$-RHOGIC. (i,j) The corresponding elemental mappings of (i) $FeCl_3$-LOGIC and (j) $FeCl_3$-HOGIC.
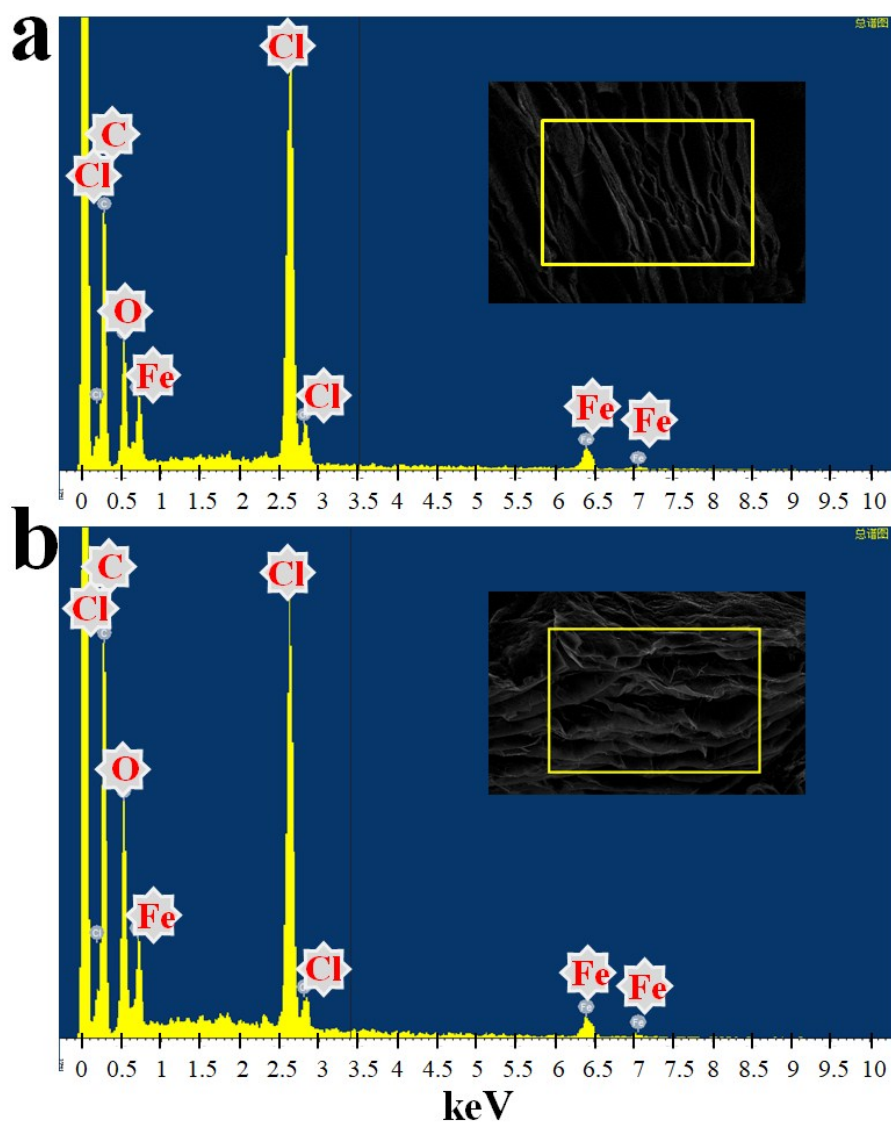
Figure S7. EDS of (a)FeCl$_3$-LOGIC and (b)FeCl$_3$-HOGIC.

Oxygen atomic percentages of FeCl$_3$-LOGIC and FeCl$_3$-HOGIC are 11.4%, 15.1%, respectively.
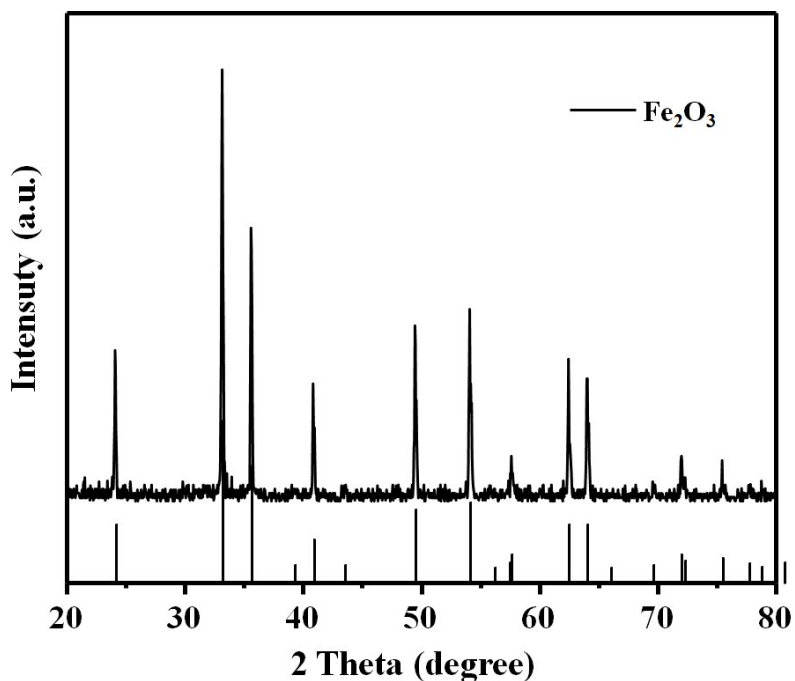
Figure S8. XRD pattern of the thermal analysis product in air.

Table S1. The $FeCl_3$ contents in pristine graphite (G) and various $FeCl_3$-based GICs.

Sample	G	$FeCl_3$-GIC	$FeCl_3$-LOGIC	$FeCl_3$-HOGIC	$FeCl_3$-RHOGIC
$FeCl_3$ contents	0.00%	60.7%	58.1%	51.8%	46.1%

The $FeCl_3$ contents were measured by thermal analysis in air. The various GICs and graphite were heated at 900 °C for 2 h in a muffle furnace. The final product can be indexed to Fe_2O_3 after heating from the XRD result (Figure S8).[2] Based on the change in weight and conversion ratio, the contents of $FeCl_3$ in different GICs are estimated and results are shown in Table S1.
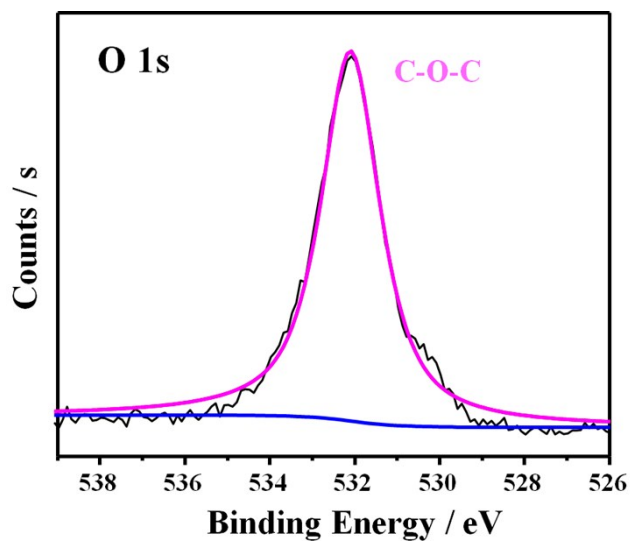
Figure S9. XPS profiles of the high-resolution spectra of O 1s of the FeCl$_3$-HOGIC.
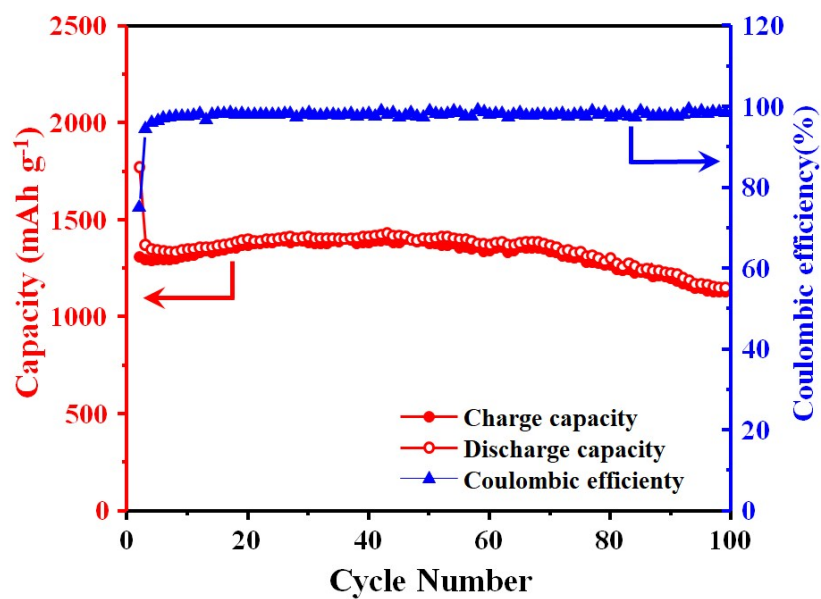
Figure S10. Long cycle performance of FeCl$_3$-HOGIC with 100 cycles.
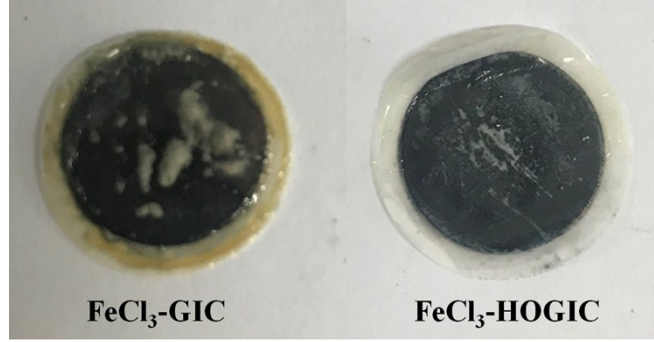
Figure S11. The photo of separator for LIBs after 50 cycles: (a) FeCl₃-GIC and (b) FeCl₃-HOGIC at a current density of 200 mA g⁻¹. The yellow color of separator from FeCl₃-GIC electrode undoubtedly comes from the dissolution of yellow FeCl₃ matter.

Calculation of the volume variation ratio in FeCl₃-HOGIC anode

To accurately calculate the volume variation ratio of FeCl₃-HOGIC after full lithiation, it is divided into two components: FeCl₃ and graphite. Their parameters are shown in the following table:

Component	ρ, Density (g cm⁻³)	ω, Weight ratio	ΔV, Volume variation ratio
FeCl₃	2.90	51.8%	22.6%
graphite	2.25	48.2%	10.5%

Considering the total mass of FeCl₃-HOGIC is m, The volume variation ratio of FeCl₃-HOGIC can be calculated using the following equation:

$$\Delta V = \frac{(m\omega_{(FeCl_3)} / \rho_{(FeCl_3)}) \times (\Delta V_{(FeCl_3)} + 1) + (m\omega_{(graphite)} / \rho_{(graphite)}) \times (\Delta V_{(graphite)} + 1)}{m\omega_{(FeCl_3)} / \rho_{(FeCl_3)} + m\omega_{(graphite)} / \rho_{(graphite)}} - 100\%$$

Therefore, $\Delta V_{(FeCl3-HOGIC)}$ = (0.518m/2.90 × 1.226 + 0.482m/2.25 × 1.105) / (0.518m/2.90 + 0.482m/2.25) 100% = 16.0%
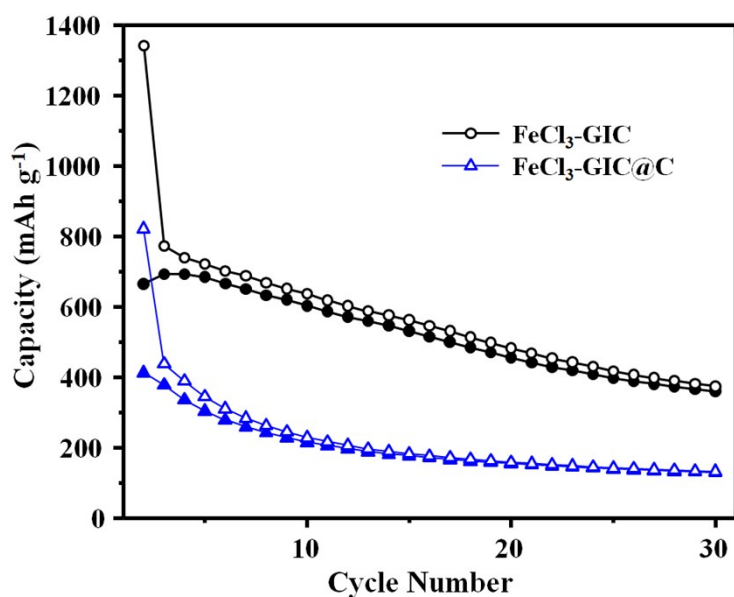
Figure S12. Cycle performance of FeCl$_3$-GIC and FeCl$_3$-GIC@C at a current density of 200 mA g^{-1}.

Preparation of FeCl$_3$-GIC@C.

The carbon coating procedure of FeCl$_3$-GIC was performed using our previously reported method.[3] 280 mg of FeCl$_3$-GIC precursor was dispersed in 100 mL of Tris buffer aqueous solution (pH: ~8.5) and subsequently 100 mg of dopamine was added. The polymerization was occurred at 35 °C for 24 h under continuous stirring. Afterwards, the collected polydopamine-coated FeCl$_3$-GIC was heated at 3 °C min^{-1} from room temperature to 150 °C and kept at this temperature for 1 h under an argon flow. The temperature was then raised at 1 °C min^{-1} to 450 °C and kept at this temperature for 4 h to achieve the FeCl$_3$-GIC@C material.
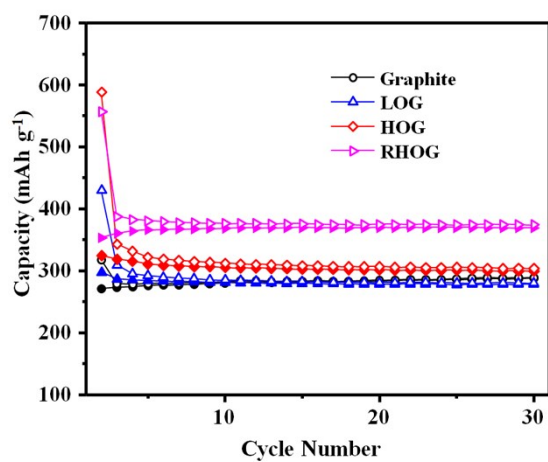
Figure 13. Comparison of cycle performance of pristine graphite, LOG, HOG and RHOG at a current density of 200 mA g^{-1}.

	C$_6$Li	CLi	
	a	**b**	Top view
			Side view
Binding energy	E_{b1}= 2.32eV	E_{b2}= -0.39eV	
	CLi/FeCl$_3$	CLi/LiCl	
	c	**d**	Top view
			Side view
Binding energy	E_{b3}= 3.74eV	E_{b4}= 2.67eV	

Figure S14. The structural models and simulated formation energies of (a) C$_6$Li, (b) CLi, (c) CLi/FeCl$_3$ and (d) CLi/LiCl with top view and side view structures.

The formation energy per Li atom (E_b) for the thermodynamic stability of a graphite layer with the monolayer Li to make C$_x$Li composite or CLi with the monolayer FeCl$_3$ and LiCl, are defined as:
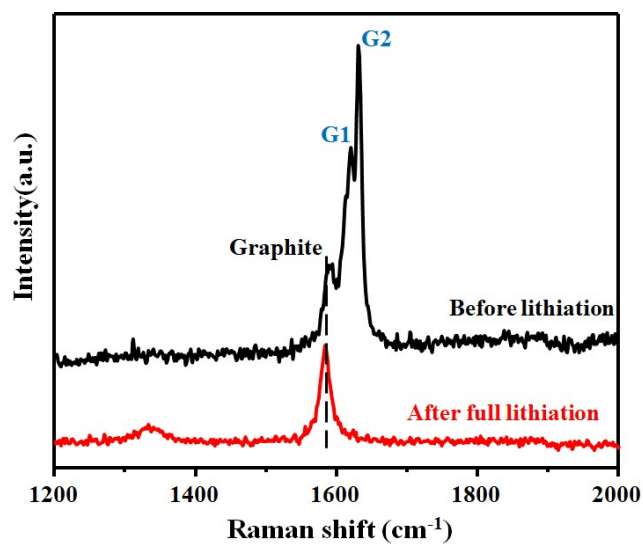
$$E_{b1}=(E_{Li}+ E_G - E_{C_6Li})/n$$

$$E_{b2}=(E_{Li}+ E_G - E_{CLi})/n$$

$$E_{b3}=(E_{FeCl_3}+ E_{CLi} - E_{CLi/FeCl_3})/n$$

$$E_{b4}=(E_{LiCl}+ E_{CLi} - E_{CLi/LiCl})/n$$

where E_{Li}, E_{LiCl}, E_G, E_{C_6Li}, E_{CLi}, $E_{CLi/FeCl_3}$ and $E_{CLi/LiCl}$ represent the total relaxation
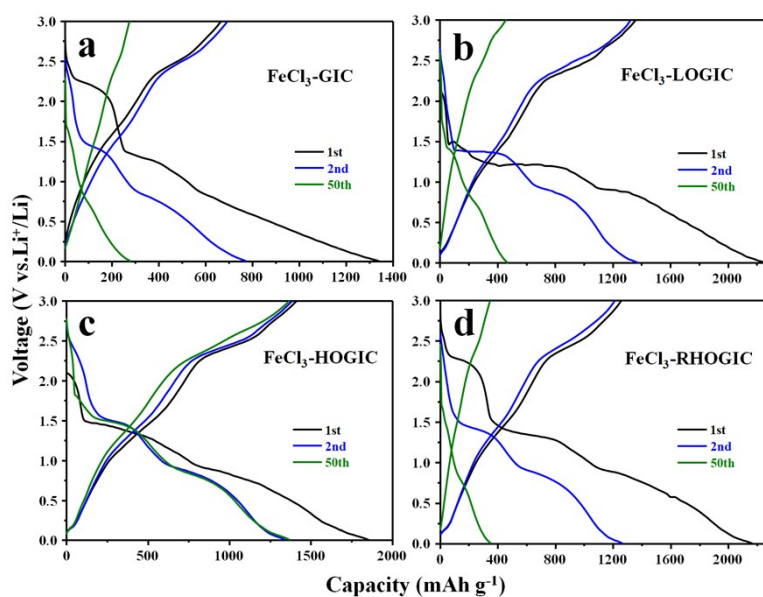
energies of monolayer Li, LiCl, G, C_6Li, CLi, $CLi/FeCl_3$ and CLi/LiCl composite, respectively. *n* is the total number of Li atom in the supercell.

Figure 15. Raman spectra of $FeCl_3$-HOGIC before lithiation and after the full lithiation to 0.005 V.
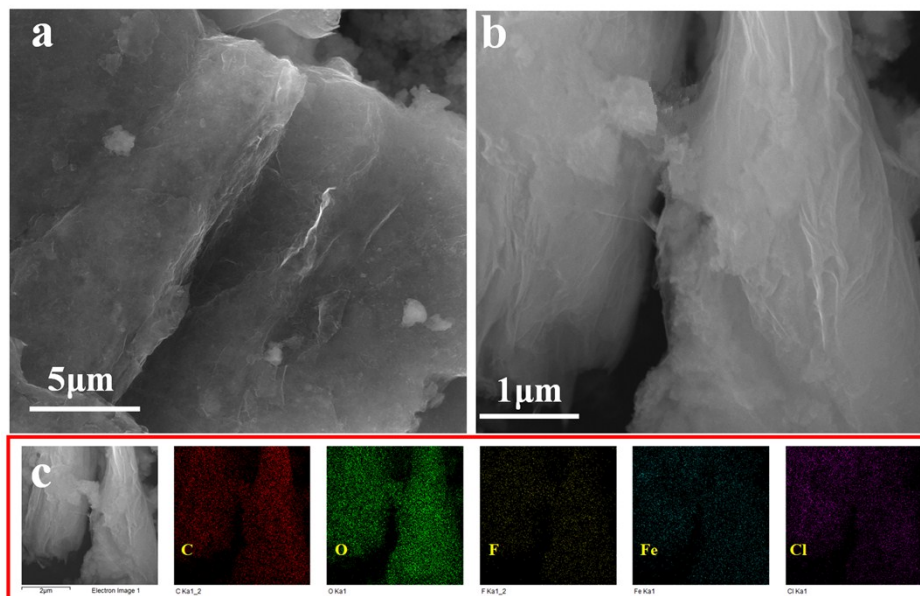
Figure S16. The SEM images of FeCl$_3$-HOGIC anodes after 50 fully charge/ discharge cycles and (c) the corresponding elemental mappings.
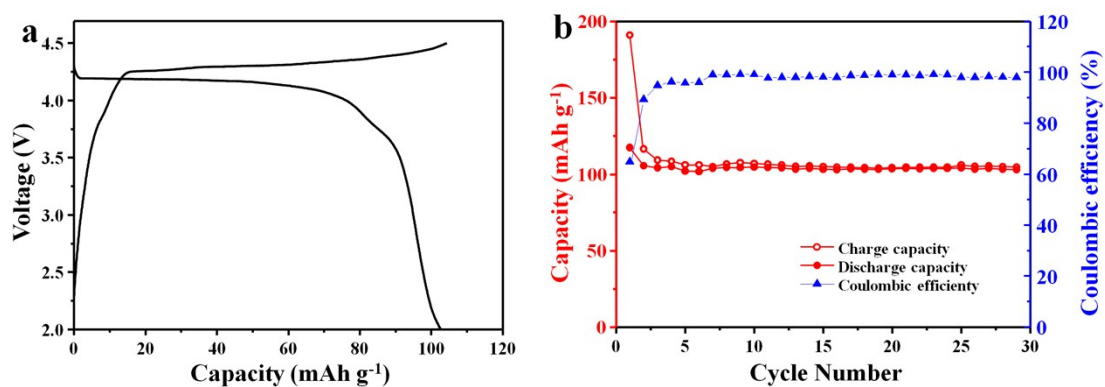

Figure S17. Galvanostatic discharge/charge profiles of (a) FeCl$_3$-GIC, (b) FeCl$_3$-LOGIC, (c) FeCl$_3$-HOGIC and (d) FeCl$_3$-RHOGIC at a current density of 200 mA g^{-1} within the potential window of 3.0 to 0.005 V.

Table S2. Fitted electrochemical impedance parameters of the FeCl₃-HOGIC anode.

Sample	R_e/Ohm	R_f/Ohm	R_{ct}/Ohm	Z_w/Ohm
fresh	4.28	113.26	157.54	41.34
after 1st cycle	5.34	6.74	15.26	63.57
after 50th cycle	9.42	5.57	14.84	78.91

Figure S18. (a) Typical galvanostatic discharge/charge profiles of a full cell consisting of LiVPO₄F cathode and FeCl₃-HOGIC anode between 2.0 and 4.5 V and (b) its cycle performance and Coulombic efficiencies.
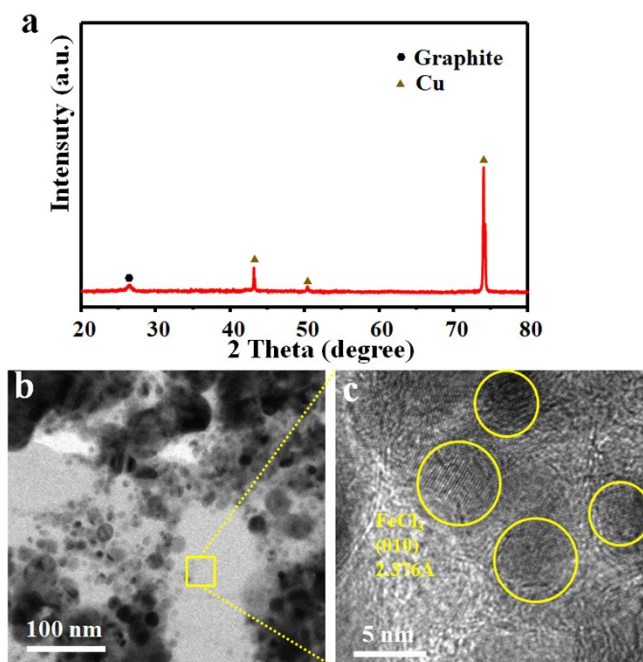
Figure S19. (a) XRD pattern and (b,c) TEM images of the FeCl$_3$-HOGIC electrode after 50 cycles at a current density of 200 mA g^{-1}.

References

1. Z. Tian, P. Yu, S. E. Lowe, A. G. Pandolfo, T. R. Gengenbach, K. M. Nairn, J. C. Song, X. Wang, Y. L. Zhong and D. Li, *Carbon*, 2017, 112, 185-191.
2. F. Wang, J. Yi, Y. Wang, C. Wang, J. Wang and Y. Xia, *Adv. Energy Mater.*, 2014, 4, 1300600.
3. F. Han, C. Zhang, J. Yang, G. Ma, K. He and X. Li, *J. Mater. Chem. A*, 2016, 4, 12781-12789.